URSI-RCRS 2024, ARIES/GEHU, Bhimtal, India, 22 - 25 October, 2024

Design of Compact Multiband Circular Patch Antenna with E slot for Medical Microwave Radiometry

Neenu Vymeliyath Sajeev, and Kavitha Arunachalam
Department of Engineering Design, Indian Institute of Technology Madras, India

Abstract

This paper presents the design and analysis of a compact multiband circular microstrip patch antenna with an E slot operating over 1 to 5 GHz for medical microwave radiometry applications. A miniaturized near-field circular patch antenna of 24 mm diameter with superstrate is reported for brightness temperature measurement. The introduction of E slot on the circular patch introduced three resonances at 1.56, 2.42, and 4.64 GHz with return loss more than 10 dB and bandwidth greater than 100 MHz in each band. Furthermore, the antenna has localized power deposition in tissue at the resonance frequencies. The simulation study indicates that this multiband antenna has spatially varying sensing volumes with penetration depth varying over 15 to 26 mm, which could be used to estimate the depth of thermal anomaly.

1. Introduction

Accurate measurement of deep tissue temperature is critical in various medical applications such as temperature monitoring during hyperthermia treatment, and diagnosis of inflammatory conditions, mostly tumors. Conventional techniques such as thermocouples, infrared thermography, and magnetic resonance imaging provide valuable insights but often face limitations regarding sensitivity and penetration depth. Microwave radiometry (MWR) offers a passive and non-invasive method for measuring the temperature of deep tissues [1]. The principle behind this method is to gather thermal emission from tissues in electromagnetic (EM) spectrum as a function of their temperature using a microwave radiometer and provide the brightness temperature of tissues located deep underneath the skin. Figure 1 illustrates the MWR setup typically used for passive tissue thermometry.

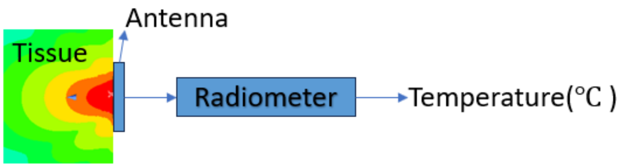

Figure 1. Illustration of microwave radiometry (MWR) for passive deep tissue thermometry

EM radiation emitted by the tissue under investigation is received by an impedance matched antenna in contact with the tissue and processed by the [1] radiometer to estimate the tissue temperature. It is very challenging to design a well-matched near-field antenna so that the ultra-low power radiation emitted by tissues are received by the radiometer with minimum power reflection and maximum power gathering efficiency from deep lying tissues to improve accuracy and penetration depth of the radiometer measurements.

There are several near field antennas reported for medical MWR. Measurement of deep brain temperature in newborn infants using a multifrequency radiometer was reported in [2] along with temperature-depth profile retrieval algorithm using model fitting and Monte Carlo techniques. A single band body contacting substrate integrated waveguide resonant antenna at 1.3 GHz excited by a tapered feed line with defective ground was reported to measure deep-seated thermal anomalies [3]. Resonant near field probe-fed microstrip patch antenna with improved measurement sensitivity and sensing depth up to 4 cm was reported in [4]. Ultrawideband Archimedean spiral antenna was reported for multi-band MWR to provide additional insights on the depth of tissue thermal anomaly [5]. Ultrawideband antennas reported for medical MWR are prone to ambient EM interference and requires shielding for stable operation [6]. Thus, multi-band antennas are desired for multi-frequency MWR.

In this paper, design and analysis of a miniaturized three-band circular microstrip patch antenna is presented for medical MWR. A circular patch with E shaped slot is optimized for three resonance bands over 1 to 5 GHz. The numerical design and analysis show that the three-band antenna has varying near field power reception characteristics, which could be used to estimate the depth of tissue thermal anomaly while analyzing brightness temperature measurements gathered using a three-band microwave radiometer.

2. Principle of microwave radiometry

Every object above 0 K emits EM radiation and the noise power of the thermal radiation is given by [7],

$$P = kT_sB, \tag{1}$$

where k is the Boltzmann constant, T_s is the absolute temperature of the source, and B is the bandwidth of noise power measurements. In MWR, thermal radiation emitted by biological tissues is measured by a microwave radiometer that yields the brightness temperature (T_b) which is related to tissue steady state temperature distribution, $T(r)$ by [4],

$$T_b = \int_V W(\vec{r}, f)\, T(\vec{r})\, dV. \qquad (2)$$

In Eqn. (2), W is the antenna weighting function defined over the sensing volume, V of the receive antenna at the measurement frequency, f. The frequency dependence of brightness temperature arises from W, which is related to the antenna volume power loss density (VPD) [4],

$$P_d(\vec{r}, f) = \frac{1}{2}\sigma(\vec{r})\left|\vec{E}(\vec{r}, f)\right|^2. \qquad (3)$$

In Eqn. (3), σ is the tissue electrical conductivity, $\vec{E}$ is the electric field intensity and $\vec{r}$ is the position vector. The normalized VPD inside the antenna sensing volume yields, W expressed in Eqn. (4).

$$W = \frac{P_d(\vec{r}, f)}{\int_V P_d(\vec{r}', f)\, dV} \qquad (4)$$

Due to reciprocity, antenna weighting function in receive mode is calculated by analyzing the antenna in transmit mode [2, 4, 7]. As tissues are lossy dielectrics, the sensing volume of the antenna decreases with increase in frequency. As a result, noise power from deep lying tissues can be gathered at lower frequency compared to higher frequency. In multi-frequency MWR, measurements gathered at different frequencies are analyzed to estimate the depth from the brightness temperature measurements [2, 7].

3. Multiband antenna design

A microstrip patch with E slot was designed using HFSS simulation software (Ansys, Pittsburgh, USA) for multiband resonance. Figures 2(a) and 2(b) show the top and side views of the antenna with patch radius, r_p and ground radius, r_s. The dimensions of the E slot namely, width (S_w), slot length (S_l) and distance between two edge arms, d were optimized using parametric sweeps to obtain three resonances over 1-5 GHz. The operating frequency range of 1 to 5 GHz was selected as it is widely reported for multi-frequency medical MWR [2]. The patch was excited by a coaxial pin at position (f_x, f_y) through 2.54 mm thick Rogers RT/Duroid 6010 (Rogers. Corp., USA) substrate with dielectric constant 10.2. The VPD in tissue was enhanced using a superstrate made of Rogers RT/Duroid 6006 laminate with dielectric constant 6. The superstrate improved antenna impedance matching to tissue which in turn improved sensing volume and gathered noise power from tissue. Figure 2(c) shows the three dimensional (3D) model of the patch antenna on a muscle equivalent tissue with dielectric constant of 39.32 and conductivity of 0.26 (S/m) at 5 GHz [4]. The computational domain in Figure 2(c) was terminated with absorbing boundary condition and coaxial feed was excited with swept frequency source. Material properties of Rogers laminates inbuilt in HFSS were assigned for the antenna. Frequency dependent tissue properties reported in [4] was used for antenna design.

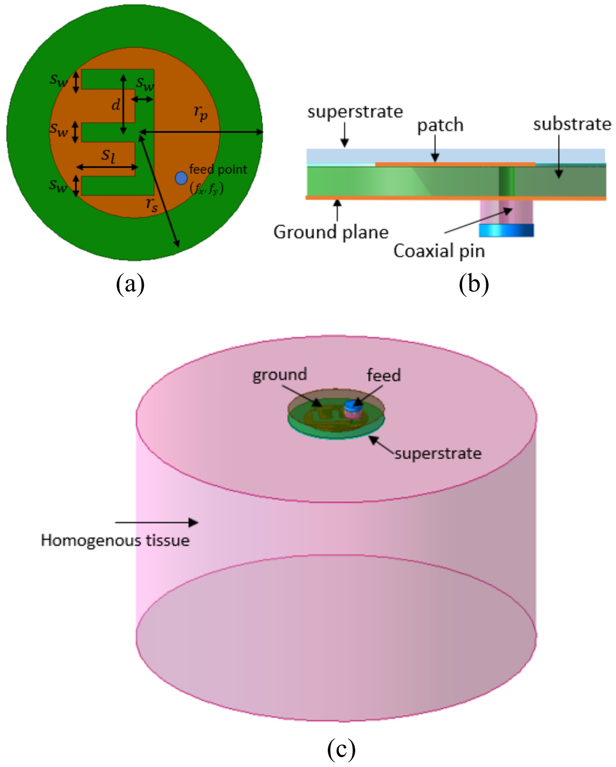

Figure 2. Antenna numerical modeling. (a) Top and (b) side views of the E slot circular patch antenna, (c) 3D model with homogenous tissue.

The patch with slot dimensions and optimal superstate thickness that satisfied the following design criteria was used for further analysis: (i) three resonances between 1 and 5 GHz, (ii) power reflection coefficient, $|S_{11}|^2$ below -10 dB at each resonance frequency with, (iii) -10 dB bandwidth of at least 100 MHz at the individual resonance band.

Table 1. Antenna design parameters

Antenna parameters	Optimized value
Ground radius (r_s)	12 mm
Patch radius (r_p)	8 mm
E slot width (S_w)	1.8 mm
E slot length (S_l)	5 mm
E slot gap (d)	5 mm
Substrate permittivity	10.2
Substrate thickness	2.54 mm
Superstrate permittivity	6
Superstrate thickness	0.254 mm
Feed point (f_x, f_y)	(4, 4) mm

4. Numerical analysis

The final design parameters of the circular patch antenna with E slot are given in Table I. The return loss of the miniaturized multi-band circular patch antenna with E slot is shown in Figure 3. Figure 3 shows resonance at $f_1 = 1.56$ GHz, $f_2 = 2.42$ GHz and $f_3 = 4.64$ GHz with $|S_{11}|^2$ below -10 dB and bandwidth greater than 100 MHz in each band. Thus, the circular patch with the optimized E slot design parameters satisfied the antenna design criteria for tissue MWR.

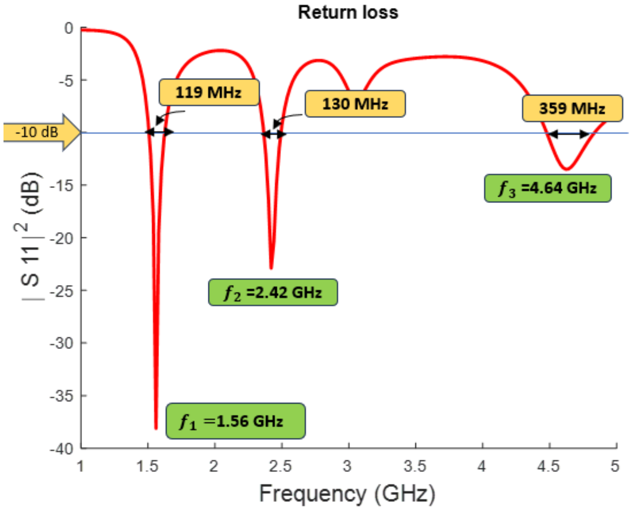

Figure 3. Power reflection coefficient of the circular patch with optimized E slot.

Antenna electrical performance at the three resonance frequencies, f_r is summarized in Table II.

Table II. Antenna electrical performance

f_r (GHz)	$\lvert S_{11}\rvert^2$ (dB)	Bandwidth (MHz)	Mode
1.56	-38	119	TM_{11}
2.42	-23	130	TM_{21}
4.64	-14	359	TM_{31}

The surface current density (J_{surf}) and electric field intensity $(\vec{E})$ on the patch at three frequency bands are shown Figure 4. Addition of E slot on the patch lowered the 2.6 GHz resonance frequency of the simple circular patch to 1.56 GHz due to increase in the current path length. The slot also introduced higher order resonance modes. Figure 4(a) shows that at 1.56 GHz, maximum current is about the edges of the patch due to the perturbation introduced by the E slot. Figure 4(b) shows that the maximum electric field intensity is occurring radially across the edges of the patch confirming fundamental TM_{11} mode at 1.56 GHz. Figures 4(c) and 4(d) show the current density and electric field distribution at 2.42 GHz due to TM_{21} mode with two minima along the radial direction. Figures 4(e) and 4(f) shows the influence of the slot at 4.64 GHz on patch current density and electric field distributions with three nodal points along the radial direction which presents a TM_{31}mode of the antenna.

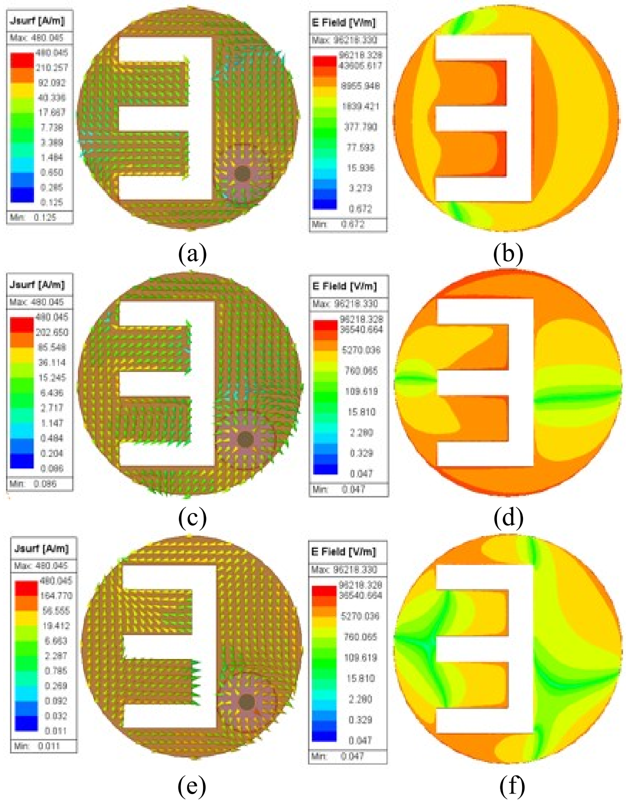

Figure 4. Electric field and current distribution on the optimized patch. (a) $\vec{J}_{surf}$ at f_1 (b) $\vec{E}$ at f_1 (c) $\vec{J}_{surf}$ at f_2 (d) $\vec{E}$ at f_2 (e) $\vec{J}_{surf}$ at f_3 (f) $\vec{E}$ at f_3.

Figure 5 shows the VPD in tissue orthogonal planes along the depth. VPD determines the spatial coverage of the power received from deep tissues by an antenna when the reciprocity of antenna is taken into consideration. In this study, the -15 dB power level computed for the normalized VPD in transmit mode was used to calculate the penetration depth in tissue. Thus, VPD profiles in Figure 5 demonstrate the normalized power reception capability of the antenna from the tissue in the two orthogonal depth planes (XZ, YZ). The VPD depends on tissue dielectric property and electric field intensity induced on the receive antenna. Figure 5(a) shows VPD profile at 1.56 GHz in both YZ and XZ planes. The penetration depth that corresponds to -15 dB is 12 mm. Figure 5(b) shows the VPD profile at YZ and XZ plane at 2.42 GHz which has penetration depth of 26 mm due to a higher concentrated electric field present in TM_{21} mode. At 4.64 GHz, electric field strength is much more concentrated than the uniform electric field at 1.56 GHz, but compared to TM_{21} mode. The penetration depth is 15 mm at 4.64 GHz which is lower than 26 mm calculated for 2.42 GHz. It should be noted that unlike plane wave illumination which dictates increase in penetration depth with decrease in frequency, the penetration depth for the E slot patch at 1.56 GHz is lower than at 2.42 and 4.64 GHz as the EM field maintained by the microstrip patch is not that of a plane wave source.

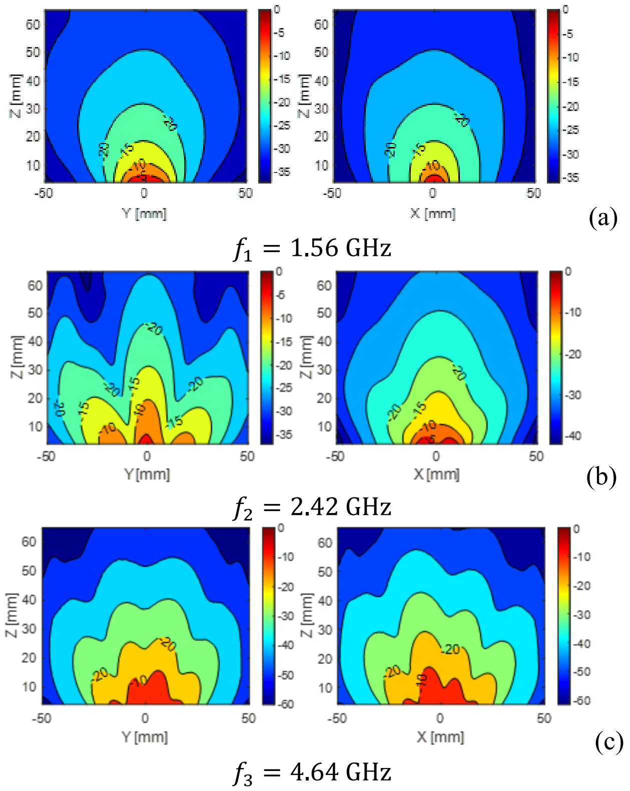

Figure 5. Volume power loss density. (a) at 1.56 GHz in YZ and XZ plane (b) at 2.42 GHz in YZ and XY plane (c) at 4.64 GHz.

Figure 6 shows the one-dimensional depth profiles of VPD along the antenna broadside at 2.42 and 4.64 GHz. From Figures 5 and 6, it can be observed that brightness temperature gathered by the E-slot patch at 2.64 and 4.64 GHz frequency bands could be used to retrieve depth information of the thermal anomaly using a dual band microwave radiometer.

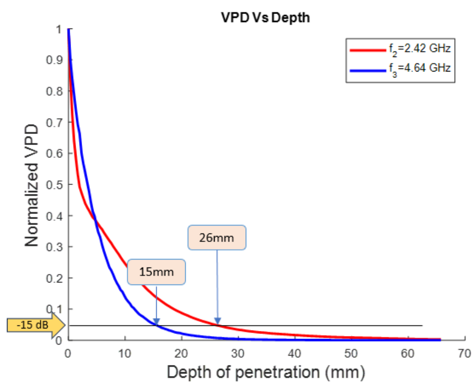

Figure 6. Penetration depth at two measurement bands.

5. Conclusion

Design and analysis of a multiband circular patch antenna with E slot is presented for deep tissue radiometry. The proposed antenna resonates at 1.56, 2.42 and 4.64 GHz with return loss more than 10 dB and at least 100 MHz bandwidth in each band. The maximum penetration depth was observed to be 26 mm at 2.42 GHz. In this simulation study, it was observed that the VPD of the antenna has dependence on the modal electric field distribution of the antenna, which in turn affected the depth of penetration at resonance. Preliminary simulations of the near-field E slot patch indicate the feasibility of using multiband resonant antenna for multi-frequency medical MWR. Detailed investigations on enhancing the sensing volume of the multi-band antenna are currently under progress for extracting depth information along with tissue brightness temperature.

6. References

1. J. P. Issac and K. Arunachalam, "Design of an impedance matched near field passive antenna for medical microwave radiometry," in *2022 3rd URSI Atlantic and Asia Pacific Radio Science Meeting (AT-AP-RASC)*, 30 May-4 June 2022 2022, pp. 1-3, doi: 10.23919/AT-AP-RASC54737.2022.9814305.

2. K. Maruyma *et al.*, "Feasibility of noninvasive measurement of deep brain temperature in newborn infants by multifrequency microwave radiometry," *IEEE Transactions on Microwave Theory and Techniques,* vol. 48, pp. 2141-2147, 12/01 2000, doi: 10.1109/22.884206.

3. V. M. Ravi and K. Arunachalam, "SIW slot antenna for passive measurement of thermal anomalies in biological tissues," *IET Microwaves, Antennas & Propagation,* vol. 12, no. 7, pp. 1048-1053, 2018, doi: 10.1049/iet-map.2017.0340.

4. J. P. Issac and K. Arunachalam, "Enhanced Measurement Sensitivity Using Near-Field Antenna With MMIC Low-Noise Amplifier for Deep Tissue Microwave Thermometry," *IEEE Sensors Journal,* vol. 23, no. 15, pp. 16960-16967, 2023, doi: 10.1109/JSEN.2023.3288274.

5. S. P. Sugumar, K. Arunachalam, and C. V. Krishnamurthy, "Design of an Ultra-wide Band Active Antenna for Medical Microwave Radiometry," in *2019 URSI Asia-Pacific Radio Science Conference (AP-RASC)*, 9-15 March 2019 2019, pp. 1-3, doi: 10.23919/URSIAP-RASC.2019.8738779.

6. K. Arunachalam, P. F. Maccarini, V. De Luca, F. Bardati, B. W. Snow, and P. R. Stauffer, "Modeling the detectability of vesicoureteral reflux using microwave radiometry," *Phys Med Biol,* vol. 55, no. 18, pp. 5417-5435, 2010, doi: doi:10.1088/0031-9155/55/18/010.

7. F. T. Ulaby and D. Long, *Microwave Radar And Radiometric Remote Sensing*. Artech House, 2015.